Intercomparison of water vapor calibration constants derived from in-situ and distant soundings for a Raman-Lidar operating in the Amazon Forest

Henrique M. J. Barbosa[1], D. A. Gouveia[1], P. Artaxo[1], T. Pauliquevis[2], D. K. Adams[3], R. M. N. Santos[3]

[1] Instituto de Física, USP, São Paulo-SP, Brazil
[2] Depto. de Ciencias Exatas e da Terra, UNIFESP, Diadema, São Paulo-SP - Brazil
[3] Programa de Pos Graduacao em Clima e Ambiente, INPA/UEA, Manaus-AM - Brazil

ABSTRACT

Water vapor profiles derived from UV Raman Lidar measurement need to be calibrated. An approach based on the linear fit between the lidar uncalibrated profile and different reference profiles was used to calibrate a lidar system recently deployed to the Amazon forest. For this site, the nearest WMO operational sounding is 30 km away. The possibility of using these operational dataset is investigated. Calibration was done using: (1) collocated soundings dropped during an intensive campaign in September 2011, (2) non-collocated operational soundings for the same nights, (3) non-collocated soundings with only standard WMO GTS atmospheric levels. For collocated soundings, the derived calibration constant was 0.681 ± 0.045 (rms) ± 0.040 (inst) g/g. Initial results with no Rayleigh or Mie scattering correction show non-collocated constants to be 30% larger than collocated ones, forbidding the use of these operational soundings for periodic calibration.

1. INTRODUCTION

Recent studies have focused on the complex relation between water vapor variability and deep convection in the tropics [1]. Differently from high latitudes, rotational constrains are weak (e.g. Coriolis) and perturbations from diabatic heating are rapidly redistributed over large distances [2]. The concentration of water vapor in the tropics is highly variable in both time and space. Its vertical distribution above the boundary layer depends on slow advection and on the deep convection it self, which serves as the free troposphere's water vapor source. At the same time, deep convection itself is sensitive to the distribution of humidity in the free troposphere, developing more vigorously in humid environments, which is a positive feedback [3]. Water vapor also plays an important role in the convective available potential energy (CAPE). CAPE depends essentially on the boundary layer humidity, but also on the concentration of water in the free troposphere through virtual temperature effects [4; 5]. On the other hand, CAPE is constantly removed from the atmosphere by convection itself, which is a negative feedback that works for the stabilization of the atmosphere.

From the above discussion, it is clear that observations with high spatial and temporal resolution are necessary for a better understanding the complex interactions and feedback mechanisms between convection and humidity which occur in meso or smaller scales. There are very few such measurements on tropical regions. Indeed, there were important field campaigns in the Amazon that explored some aspects of deep convection, mesoscales systems and clouds microphysics (e.g., WETAMC and TRMM/LBA [7]). These, however, were short-intensive campaigns not allowing for a climatological perspective.

To overcome this lack of observations, a new experimental site was recently implemented near Manaus-AM, in the Brazilian Amazon Forest. The ACONVEX (*Aerosols, Clouds, cONVection EXperiment*) site will run continuously during the next years applying a synergy of different instruments, as described in section 2.1. This paper focus on the Raman-Lidar system used for measurements of water vapor and aerosol optical properties vertical distributions. Further details about the system is given in section 2.2. For reliable water vapor measurements, lidar profiles were calibrated with collocated soundings launched during an intensive campaign between in September 2011, as described in section 3. Although collocated soundings are definitely the best approach for calibrating a lidar profile, one must agree that a calibration campaign to launch ones own radiosondes is extremely time and money consuming and can only be done for a limited amount of time. Therefore, this paper compares this collocated calibration with that of an operational radiosonde performed twice a day 30 km away assuming: (1) only standard atmospheric levels; and (2) full resolution. Section 4 discuss these results and future work.

2. ACONVEX

ACONVEX intends to fill in the gap of a long time series of measurements with high spatial and temporal resolution necessary for understanding the interactions and feedback mechanisms between humidity, convection, clouds and aerosols. It was initially implemented by a partnership between different research projects: AERO-CLIMA (Direct and indirect effects of aerosols on climate in Amazonia and Pantanal), CHUVA (Cloud processes of tHe main precipitation systems in Brazil: A contribUtion to cloud resolVing modeling and to the GPM) and Amazonian Dense GNSS Meteorological Network [6].

2.1. Site Description

The ACONVEX site is located up-wind from Manaus-AM, Brazil, inside the campus of Embrapa Amazônia Ocidental, on 2.89^oS 59.97^oW. Figure 1 gives an overview of the area which is partially impacted by land use change. Instruments installed include: a meteorological weather station, a disdrometer, a multi filter shadow band radiometer, a cimel sun photometer (AERONET), a 24 Ghz micro rain radar, a ceilometer, a Trimble GNSS Receiver/Vaisla met. station and an UV Raman Lidar.
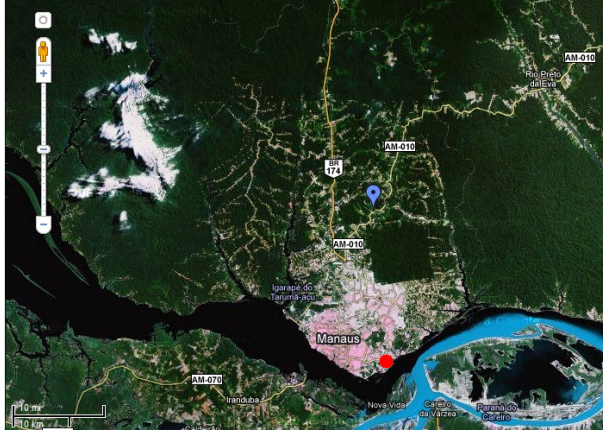
Figure 1: The location of ACONVEX site up-wind from Manaus-AM, Brazil, is indicated by the blue balloon. The red dot marks the position of the operational soundings.

2.2. UV Raman Lidar

The UV Raman Lidar is operational on the ACONVEX site since July 2011. It uses a Quantel CFR-400 Nd-YAG laser at 355 nm with 95 mJ per pulse and 10 Hz repetition rate. Beam is expanded by 3 and final laser divergence is 0.25 mrad. The optical system uses a bi-axial setup with a 400 mm separation between the cassegrain telescope and the laser axis. The telescope's primary mirror has 400 mm diameter, while the secondary has a diameter of 90 mm. Focal length is 4000 mm resulting in a f/10 system. An iris is used at the focal plane which gives a field of view of 1.75 mrad and an initial overlap at 85 m and full overlap at 450 m.

No fiber optics are used and light passing through the iris goes directly in the optical detection box. Interferometric filters separate the elastic back scattered signal and the inelastic signals due to the raman cross-section of N_2 (387 nm) and H_2O (408 nm) which are read collected in different photo-multiplier-tubes. Signals from 355 and 387 nm are recorded in analog and photon-count modes, while 408 nm only in photon count. The optical system was designed to give an uniform signal on the cathode surface almost independent of height of the detected signal. A neutral density filter is used to attenuate the elastic signal avoiding saturation, and a good signal to noise ratio (S/N) is found above 15 km depending on the atmospheric conditions. The N_2 channel, 1-min average

signals have good S/N up to 15 km but only during night time. For the H_2O channel, 1-min average signals have good S/N only up to 6 km during night time.

The system is fully automated and includes a clock-controlled shutter to cover the telescope and laser quartz windows from direct sunlight exposure between 11 am and 2 pm local time. As a backup system, a 10 mm shutter is positioned just above the iris and kept in its light-blocking position by a coil mechanism. Interlocks are connected to the UPS and to the sun light sensor, a small telescope with a 10° field of view around the large telescope axis. Environmental conditions effects on the electronics are minimized by continuously running an air conditioning and a dehumidifier inside the instrumentation cabinet.

3. WATER VAPOR MEASUREMENT

The raman lidar equation for a pulse of wavelength λ returning at a raman wavelength λ' can be written as

$$
\begin{aligned}
P(z, \lambda, \lambda') &= P_0 \frac{c\Delta T}{2} A_{tel} \eta_{eff}(\lambda') \frac{O(z)}{z^2} \beta(z, \lambda, \lambda') \\
&\quad exp\left[\int_0^z (\alpha(z', \lambda) + \alpha(z', \lambda'))dz'\right]
\end{aligned}
$$

where P_0 is the pulse energy, $c\Delta T/2$ is its length, α is the volumetric attenuation coefficient, $\beta(z, \lambda, \lambda')$ is the raman backscatter coefficient, A_{tel} is the telescope effective area, $\eta_{eff}(\lambda')$ is the detection quantum efficiency, and $O(z)/z^{-2}$ is a geometric factor.

As the atmospheric mixing ratio of N_2 is constant, it is possible to measure the mixing ratio of H_2O by taking the ratio of both background corrected signals [8], what eliminates uncertainties such as the geometrical factor. This is a well established technique [9] and results in the following expression

$$
w_{H_2O} = C\Gamma_A\Gamma_M \frac{\overline{S_{H_2O}} - \overline{BG_{H_2O}}}{\overline{S_{N_2}} - \overline{BG_{N_2}}}
$$

where the constant Γ_A and Γ_M are the differential aerosol and molecular transmission between 387 nm and 408 nm and the overbars denote temporal and spatial averages necessary for obtaining a good signal to noise ratio.

There are different approaches for solving this equation. While some authors consider C to be the callibration constant [8], some consider $C\Gamma_A$ [10], and others $C\Gamma_A\Gamma_M$ [11]. While the first approach is more precise, it is also more difficult to implement operationally. In this work, the methodology of [11] is used and hence the derived calibration constants might include some contamination of the differential Mie and Rayleigh scattering.

3.1. Calibration Constant

The calibration for measurements of water vapor profiles is still a limiting factor [10] of Raman-Lidar technique. Here the simplest approach is used, i.e., a least square
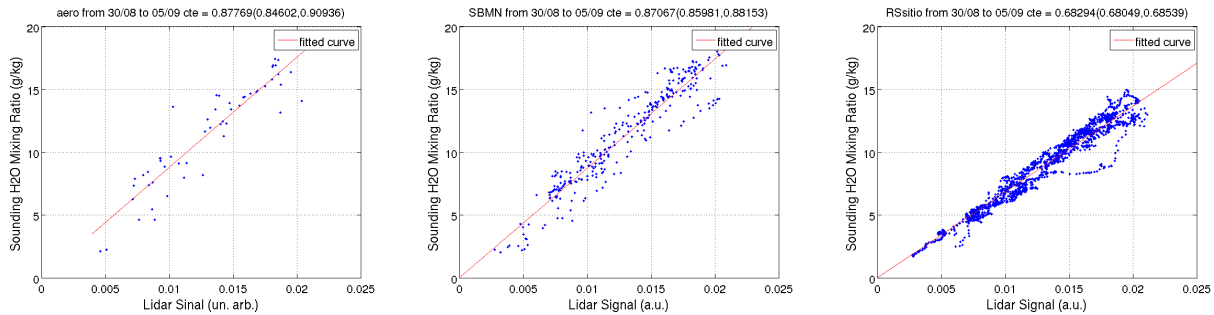
Figure 2: Panels show fitting between uncalibrated lidar profiles and reference water vapor measurements for: (left) SBMN standard levels only; (center) SBMN full resolution; (right) collocated sounding. Values between brackets are the 95% confidence limit. Fitting used all data from August 30th to September 5th 2011.

fit of $y = \alpha x$ between the uncalibrated lidar profile and independent collocated soundings. The fit uses data between 500m and 3 km because: (1) radiosondes have an accuracy of about 5% at lower altitudes, (2) the radiosonde is closer to the lidar, and (3) there is more water vapor and larger signal.

The calibration process was divided in three steps: (1) temporal and vertical average of uncalibrated lidar profiles; (2) interpolation of high resolution lidar profiles to the sounding levels; and (3) linear regression between $w_{H_2O}^{sounding}$ and uncalibrated lidar profile. The temporal and vertical smoothing are necessary for obtaining a good signal to noise ratio, but care was taken not to smooth too much and remove real variations in the water profile. The time average was varied between 3 and 30 min, and the vertical resolution between 15 to 75 m. The vertical correlation coefficient between 1 to 3 km was calculated for each profile between -100 min and +100 min of the launching time. The largest correlations were found at +8 min (i.e. ∼2 km height) when using 5 min and 30 m averages (see Fig. 3).

The calibration constant were obtained from only 8 collocated soundings performed during an intensive campaign between August 30th and 5th September 2011. For comparison, the calibration constant were also computed with the operational sounding performed twice a day, 30 km away in the Manaus military airport, the SBMN WMO station. In this case, two constants were calculated: (1) using only standard atmospheric levels as distributed via GTS; and (2) using full resolution, obtained from Brazil air-force. Only 8 operational soundings at 0Z were used, in the same nights as the collocated ones.

Figure 2 shows the fitting for the first day, a typical result. From left to right, results are SBMN at standard levels (aero); at all levels (SBMN); and the collocated sounding (RSsitio). Aero and SBMN give similar results, except for the larger 95% confidence level interval in the first case. Results from RSsitio are lower for this day and others (not shown). Values of calibration constant averaged over all sounding were 0.878±086, 0.871±058 and 0.681±0.045 g/g.

4. DISCUSSION AND FUTURE WORK

Although previous works [10] have shown it to be possible to calibrate a lidar water vapor profile from non-collocated sounding, our results indicate that it is not possible for our particular case because of the difference between the value of the calibration constant from collocated (0.681±0.045 g/g) and non-collocated soundings (0.878±086 and 0.871±058) is statistically significant.

Figure 3 shows the time series of the vertical correlation between uncalibrated lidar profile and a reference water vapor profile. There is a maximum around 2 km (8 min) only for the collocated sounding. For SBMN there is no clear pattern, what could be attributed to different advection velocities on different layers and by the proximity of the sounding site to the river and the city. The analysis of the vertical profile of the calibration constant, shown in 4, also indicates a behavior compatible with a differential advection between the 1 to 1.5 km and 1.5 to 2 km.

This analysis could depend on the range used for the vertical correlation, which was 0.5-3 km for all soundings. This was tested by varying the lower range between 0.5 and 2.5 km in 0.5 km steps, and the higher range between 2 and 5.5 km in 0.5 km steps, and repeating the correlation and calibration analysis. The 0.5-3 km range presented the highest correlations for all soundings. Moreover, the calibration constants varied by less than 5% in all cases, i.e., differences remained statistically significant.

The uncertainty in the calibration constant obtained from collocated sounding, 0.681 ± 0.045 (rms) ± 0.040 (inst) g/g, was about 6.6% rms when comparing different sounding and 5.8% instrumental. Values are larger than the 2 to 6% range indicated by [12]. Currently, work is being done to remove the contribution of molecular and aerosol scattering from the calibration constant. This might be particularly important for this region and this time of year, as September is the peak of the biomass burning season in the Amazon region.
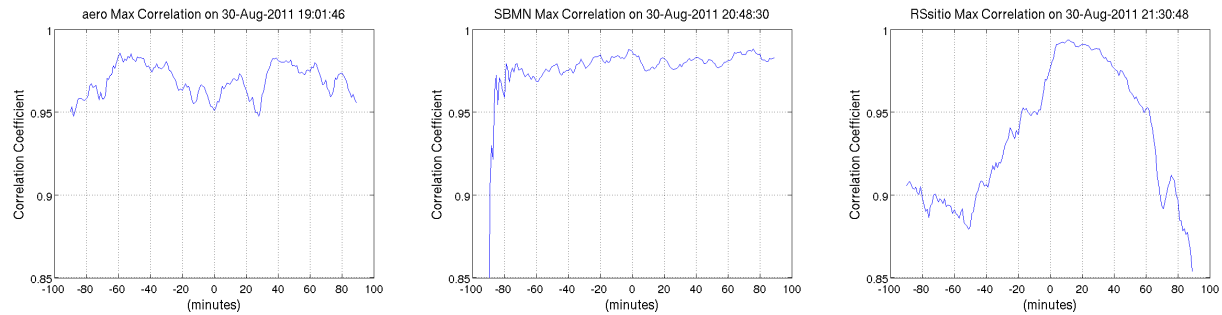
Figure 3: Panels show the lag correlation coefficient (500m-3km) between lidar profiles and reference water vapor measurements for: (left) SBMN standard levels only; (center) SBMN full resolution; (right) collocated sounding. Data from August 30th 2011.
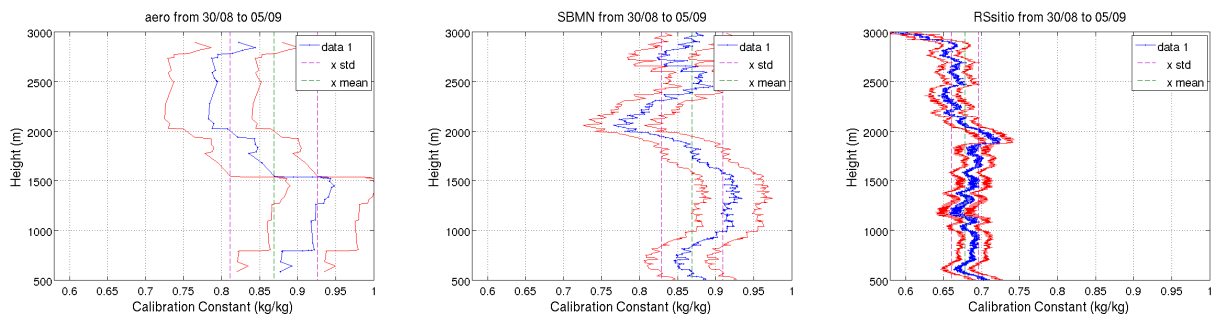
Figure 4: Panels show ratio between uncalibrated lidar profiles and reference water vapor measurements for: (left) SBMN standard levels only; (center) SBMN full resolution; (right) collocated sounding. Data shown is the average of 8 sounding between August 30th and September 5th 2011.

REFERENCES

1. Sherwood et al. 2009: Tropospheric water vapor, convection and climate: a critical review. *Review of Geophysics*, **48**, pp. RG2001.

2. Bretherton and Smolarkiewicz 1989: Gravity waves, compensating subsidence and detrainment around cumulus clouds. *J. Atmos. Sci.*, **46**, pp. 740.

3. Holloway and Neelin 2009: Moisture vertical structure, column water vapor, and tropical deep convection. *J. Atmos. Sci.*, **66**, pp. 1665.

4. Williams and Rennó 1993: An analysis of the conditional instability of the tropical atmosphere. *Mon. Weath. Rev.*, **121**, pp. 21.

5. Adams and Souza 2009: Cape and convective events over the southwest u.s. during the north american monsoon. *Mon. Weath. Rev.*, **137**, pp. 83.

6. Adams K. et al. 2011: A dense GNSS meteorological network for observing deep convection in the Amazon *Atmos. Sci. Let.*.

7. Silva-Dias et al. 2002: Cloud and rain processes in a biosphere-atmosphere interaction context in the amazon region. *J. Geo. Res.*, **107**(D20), 8072.

8. Whiteman et al. 1992: Raman Lidar system for the measurement of water vapor and aerosols in the Earths atmosphere *Appl. Opt.*, **31**(16), pp. 3068.

9. Melfi 1972: Remote measurements of the atmosphere using Raman scattering *Appl. Opt.*, **11**, pp. 1288.

10. Dionisi et al. 2010: Calibration of a Multichannel Water Vapor Raman Lidar through Noncollocated Operational Soundings: Optimization and Characterization of Accuracy and Variability *J. Atmos. Oceanic Technol.*, **27**, pp. 108.

11. Bosser et al. 2010: A case study of using Raman lidar measurements in high-accuracy GPS applications. *J. Geod.*, **84**, pp. 251.

12. Revercomb et al. 2003: The ARM programs water vapor intensive observation periods *BAMS*, **84**(2), pp. 217.